

# Reports

## Solar Cycle Variation of Exospheric Temperatures on Mars and Venus: A Prediction for Mariner 6 and 7

**Abstract.** Calculations have been made to determine the effects of variations in the extreme ultraviolet solar radiation on the upper atmospheres of Mars and Venus. The results indicate that the exospheric temperature on Mars varies from 300°K to 600°K during the solar cycle, with a corresponding range on Venus of 450°K to 850°K. At the present time, the temperature of the Martian exosphere should be approximately 500°K.

The Mariner missions to Mars and Venus provide the opportunity to measure certain properties of the upper atmospheres of these planets. However, each mission samples a particular region of the atmosphere, at a specific latitude and longitude and at a specific phase of the 11-year solar cycle. Thus, the Mariner probes may not reveal general characteristics of Mars or Venus. Nevertheless, they provide sufficient information for a determination of the general characteristics when the observations are combined with theoretical studies of atmospheric structure.

We have described a method for calculating the structure of a planetary atmosphere rich in CO<sub>2</sub> (1, 2). Using this method, we were able to reconcile the Mariner 4 and 5 observations of the atmospheres of Mars and Venus with a single set of assumptions about the basic properties of a CO<sub>2</sub> atmosphere. We now report on how those earlier calculations have been extended to obtain the variation of properties of the upper atmospheres on Mars and Venus during the entire 11-year cycle of solar activity. We have also calculated the thermal structure of the Martian atmosphere for the particular conditions anticipated for the forthcoming Mariner 6 and 7 occultations of Mars.

One of the most important parameters which can be derived from thermal calculations is the temperature of a planetary exosphere—the low-density, outermost region of the atmosphere where molecular collisions are rare. The exospheric temperature ( $T_E$ ) is of particular interest because it controls

the rate of escape of the various atmospheric constituents; hence, the study of the evolution of the atmospheres of Mars, Venus, and Earth depends upon a knowledge of this quantity. In addition,  $T_E$  is related to the falloff of density at high altitudes and thus is an important input parameter for calculations of atmospheric drag on orbiting spacecraft.

The exospheric temperature is determined from the interaction of the extreme ultraviolet (EUV) solar flux with constituents of the upper atmosphere. Since the strength of the EUV flux varies significantly (perhaps by a factor of 4) during the 11-year solar cycle, an appreciable variation of  $T_E$

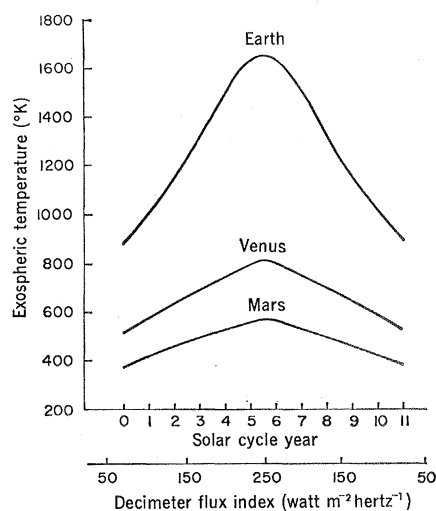


Fig. 1. Variation of the exospheric temperatures of Mars, Venus, and Earth over the solar cycle. Abscissas for all points are taken from the lower scale (decimeter flux index).

during this cycle must also occur. Because of an extremely strong dependence on  $T_E$ , the escape rate is much larger during the periods of high solar activity than during solar quietude; thus the average escape flux over long periods is determined chiefly by the high exospheric temperatures occurring near solar maximum. Therefore, an understanding of the time variation of  $T_E$  is required for a quantitative study of the evolution of planetary atmospheres.

With this motivation we have derived the variation of exospheric temperatures on Mars and Venus with solar cycle. The results are presented in Fig. 1, where the corresponding variation in the diurnal average of  $T_E$  for low and middle latitudes on Earth is also shown (3). The curve for Mars represents a day-night average for conditions on the equator at the equinox, whereas the curve for Venus corresponds to the subsolar point. We obtained the curves for Mars and Venus by assuming a mean orbital radius for each planet.

The upper atmosphere of Earth is considerably warmer than the exospheres of both Mars and Venus throughout the solar cycle, although the orbit of Earth lies at an intermediate distance from the sun. Although the atmospheres of Mars and Venus have similar composition (largely CO<sub>2</sub>), the Venus exosphere is warmer than the upper atmosphere of Mars because of the closer proximity of Venus to the sun. The exospheric temperature is higher on Earth than on either Mars or Venus because of the scarcity of CO<sub>2</sub> or other effective radiators in the terrestrial upper atmosphere.

Significant features of the upper atmosphere of Mars to be observed during the forthcoming Mariner encounters include the exospheric temperature, the peak electron density, and its altitude. Calculated values for these three parameters at the Mariner 6 and 7 occultation entry points (4, 5) are presented in Table 1, along with earlier values for the Mariner 4 and 5 encounters.

The values of  $T_E$  (Table 1) for the forthcoming occultations on Mars are considerably higher than the value of  $295^\circ \pm 28^\circ\text{K}$  calculated for the Mariner 4 encounter. The reasons for this are as follows. (i) The increased solar activity at the present time corresponds to a 100 percent increase in the solar EUV flux over its value in

July 1965, the time of the Mariner 4 encounter. (ii) Mars is now some 12 million miles nearer to the sun than at the time of the Mariner 4 occultation and is receiving an effective increase of 20 percent in solar flux due to its present position. (iii) The portions of the Martian atmosphere above the Mariner 6 and 7 occultation points will be heated by the sun for larger fractions of the day (0.59 and 0.73, respectively) than was the region above the Mariner 4 occultation point (0.52). Moreover, Mariner 7 will sample the summer hemisphere at high latitudes, where the average insolation is greater than in the equatorial region to be sampled by Mariner 6; thus we obtained a higher value of  $T_E$  in the case of Mariner 7. The longer periods of irradiance at the Mariner 6 and 7 occultation points correspond to increases over the Mariner 4 value of 13 percent and 41 percent, respectively, in the effective solar flux. It is possible, however, that horizontal energy transport, not considered here, could smooth out the temperature differences between the Mariner 6 and 7 occultation points obtained from the present one-dimensional model.

The height of the Martian ionosphere at each point on the globe depends on the temperature of the atmosphere and of the ground below. Although an estimate of the ground temperature on Mars at the occultation points can be made from radiometric data, it is not possible to predict surface conditions for these points with high accuracy. The lower atmosphere of Mars must be in near radiative equilibrium, because of strong transfer in the  $\text{CO}_2$  bands at  $15 \mu$  (6). Therefore, the choice of a boundary temperature will significantly affect the atmospheric structure below the mesopause and thus the level at which the ionosphere will develop (7). We have chosen  $280^\circ \pm 20^\circ\text{K}$  and  $260^\circ \pm 20^\circ\text{K}$  as representative of the ranges within which the ground temperature at the occultation points should lie. The corresponding ranges in the altitude of the ionization maximum  $Z_p$  are given in Table 1, along with an estimate of the peak electron density at the occultation points. An increase or decrease of  $5^\circ\text{K}$  in the assumed ground temperature produces a change in the height of the peak electron density of approximately 1 km. The effect of variations in ground temperature on the exospheric temperature is negligible, since  $T_E$  is deter-

Table 1. Calculated and observed\* properties of the upper atmospheres of Mars and Venus.

Spacecraft	Exospheric temperature ( $^\circ\text{K}$ )		Peak electron density ( $\times 10^6 \text{ cm}^{-3}$ )		Altitude of ionization maximum (km)	
	Calculated†	Observed	Calculated	Observed	Calculated	Observed
Mariner 4 (Mars)	$295 \pm 28$		0.89	$0.90 \pm 0.1$	119	$120 \pm 5$
Mariner 5 (Venus)	$648 \pm 71$	$650 \pm 50$	5.4	$5.5 \pm 0.5$	142	140‡
Mariner 6 (Mars)	$480 \pm 50$		1.3		$148 \pm 4$	
Mariner 7 (Mars)	$495 \pm 55$		1.4		$143 \pm 4$	

\* See (12). † See (13). ‡ See (14).

mined almost entirely by the balance between energy sources and sinks above the mesopause.

These results were obtained from the numerical solution of a time-independent equation for energy balance in the atmosphere. Consistent profiles of neutral particle density and electron-ion concentration were obtained by an iterative procedure (1).

The term representing the solar energy source in these calculations includes contributions from solar x-ray, EUV, near-ultraviolet, and near-infrared radiations and is evaluated by a consideration of all appropriate efficiency factors and relevant relaxation processes. The choice of the photo-ionization heating efficiency  $\epsilon$  determines the strength of the interaction of the EUV flux with the upper atmosphere and therefore exerts a direct control on the exospheric temperatures. The values of  $\epsilon$  adopted in the calculation for Mars and Venus (Fig. 1), derived from the analysis of spacecraft data (1), were 0.35 and 0.27, respectively.

The data of Hinteregger *et al.* (8) were used to obtain the intensity of the EUV (wavelength  $< 1100 \text{ \AA}$ ) solar flux at desired points in the solar cycle. Those data refer to the flux incident at the top of the atmosphere of Earth at a time near solar minimum (July 1963) and must therefore be adjusted both for the orbital radii of Mars and Venus and for variations of solar activity. Roemer (9) has shown that the EUV flux is best correlated with the decimeter flux index  $\bar{F}$ , a 5-month average of the solar decimeter (10.7 cm) flux about a given time. A range in  $\bar{F}$  of 70 to 250 (in units of  $10^{-22} \text{ watt m}^{-2} \text{ hz}^{-1}$ ) is typical of a solar cycle (10), and, in order to obtain the variation of EUV flux with solar activity, we have assumed that the EUV flux is proportional to  $\bar{F}$ .

At the time when the EUV flux data were obtained,  $\bar{F}$  was 82.6. On the basis of the sun's behavior during the present solar cycle (10), we estimate that

a decimeter flux index of about 135 will prevail at the time of the Mariner observations, and we have multiplied the Hinteregger EUV data by a factor of 1.63 to correct for the increased solar activity. The flux values employed in the calculations corresponding to the forthcoming occultations have been multiplied by a factor of 0.493 to account for the diminution of the EUV flux between the orbits of Earth and Mars (5).

Because of the rapid rotation of Mars, the response time of the upper atmosphere to variations in the solar EUV flux is probably shorter than the length of the Martian day (about 1 Earth day). For this reason, a factor  $\bar{a}$  equal to 0.59 and 0.73, respectively, for Mariner 6 and 7 is included in the solar source term to account for the diurnal variation in irradiance (11). The atmospheric response time on Venus should be of the same order. However, because of the length of the Venus day (112 Earth days), time-averaging of the solar flux is inappropriate. Therefore, the factor  $\bar{a}$  was assumed to be equal to unity in the computations for Venus.

RICHARD W. STEWART  
JOSEPH S. HOGAN

*Institute for Space Studies,  
Goddard Space Flight Center,  
National Aeronautics and Space  
Administration, New York 10025*

#### References and Notes

1. R. W. Stewart and J. S. Hogan, *J. Atmos. Sci.* **26**, 330 (1969).
2. J. S. Hogan and R. W. Stewart, *ibid.*, p. 332.
3. *COSPAR International Reference Atmosphere* (compiled by members of COSPAR Working Group 4) (North-Holland, Amsterdam, 1965), p. 98.
4. The Mariner 6 and 7 occultation entry points on Mars will be at  $6.5^\circ\text{N}$  and  $52.7^\circ\text{S}$ , respectively. In both cases, local time at the immersion point will be midafternoon (A. Kliore, personal communication).
5. On 30 July 1969 and 5 August 1969, Mars will be at a distance of 1.428 astronomical units and 1.422 astronomical units from the sun, respectively. The solar declination at that time will be approximately  $8^\circ\text{S}$  [*American Ephemeris and Nautical Almanac* (U.S. Naval Observatory, Washington, D.C., 1969)].
6. R. M. Goody and M. J. S. Belton, *Planet. Space Sci.* **15**, 247 (1967).

7. J. S. Hogan, thesis, New York University (1968); in the atmospheres of Mars and Venus, the primary maximum of ionization will develop close to the altitude at which the neutral particle density is  $2 \times 10^{10}$  particle  $\text{cm}^{-3}$ .
8. H. E. Hinteregger, L. A. Hall, G. Schmidtke, *Space Res.* **5**, 1175 (1965).
9. M. Roemer, *Veroeffentlichung Univ. Sternwarte Bonn No. 68* (1963), p. 146.
10. *Solar-Geophysical Data* (U.S. Department of Commerce, Environmental Science Services Administration, Environmental Data Service, Washington, D.C., 1969).
11. The factor  $\bar{a}$  is obtained from the expression  $\bar{a} = \omega/\pi$  where  $\omega$  is the sunset hour angle at the height of the maximum in EUV heating;  $\omega$  is related to the occultation latitude  $\phi$ , the solar declination  $\delta$ , the altitude of maximum heating  $Z_{\text{EUV}}$ , and the radius of the planet  $r$  by
- $$\omega = \arccos \frac{\cos \theta}{\cos \phi \cos \delta} - \tan \phi \tan \delta$$
- where  $\theta$  is the sunset zenith angle given by  $\theta = 90^\circ + \arccos [r/(r + Z_{\text{EUV}})]$
12. The exospheric temperature on Venus is estimated to be  $650^\circ \pm 50^\circ\text{K}$  from the Mariner 5 ultraviolet photometry data [C. A. Barth, L. Wallace, J. B. Pearce, *J. Geophys. Res.* **73**, 2451 (1968)]. A maximum electron density of  $9.0 \pm 1.0 \times 10^4$  electron  $\text{cm}^{-3}$  was observed at an altitude of about 120 km on Mars according to the Mariner 4 occultation data [G. Fjeldbo and V. R. Eshelman, *Planet. Space Sci.* **16**, 1035 (1968)]. A maximum electron density of  $5.5 \pm 0.5 \times 10^5$  electron  $\text{cm}^{-3}$  was observed at about 140 km on Venus according to Mariner 5 data [A. Kliore, G. S. Levy, D. L. Cain, G. Fjeldbo, S. I. Rasool, *Science* **158**, 1683 (1967)].
13. The spread in the calculated  $T_E$  corresponds to the range in the assumed values for the photo-ionization heating efficiency on Mars (0.25 to 0.45) and Venus (0.19 to 0.35).
14. The altitude of peak ionization on Venus is relative to a planetary radius of 6052 km. No estimate of the uncertainty in the altitude of the observed peak electron density on Venus has been published.
15. Supported by National Academy of Sciences-National Research Council associateships at the Goddard Institute for Space Studies. We thank Drs. R. Jastrow and S. I. Rasool for their advice and criticism, and Dr. A. Kliore for supplying us with the projected coordinates for the Mariner 6 and 7 occultations.

12 May 1969

## Etching Fission Tracks in Zircons

**Abstract.** A new technique has been developed whereby fission tracks can be etched in zircon with a solution of sodium hydroxide at  $220^\circ\text{C}$ . Etching time varied between 15 minutes and 5 hours. Colored zircon required less etching time than the colorless varieties.

Zircon is an ideal mineral for dating rocks by tracks caused by the spontaneous fission of  $\text{U}^{238}$ . It is a common accessory mineral in igneous, metamorphic, and sedimentary rocks; it retains fossil fission tracks at fairly high temperatures (1), and from almost any suite of zircons there would be grains with a track density suitable for counting (2) because of a wide natural range in uranium content. Routine fission-track dating of zircons has been hampered

by the difficulty of etching fossil fission tracks. Phosphoric acid has been used (2) to etch the fission tracks in zircon, but this requires high temperatures ( $375^\circ$  to  $500^\circ\text{C}$ ). Etching time is also critical. Overetch of a few seconds results in precipitation of small crystals on the surface of the zircon that obscure the fission tracks.

The etching technique described herein produces tracks (Fig. 1) similar to those developed by the phosphoric acid; however, the disadvantages of phosphoric acid technique are eliminated. The zircons ( $-60$  to  $+200$  mesh) are mounted in epoxy (3) and polished to expose an interior surface. Interior surfaces are used, as there may be fossil fission tracks on external surfaces caused by uranium in adjacent minerals. After it is polished, the epoxy mount is immersed in sodium hydroxide heated to  $220^\circ\text{C}$ . The etching solution consists of 20 g of NaOH and 5 g of  $\text{H}_2\text{O}$  (100N); the container used is a covered 35-ml platinum crucible. The mount is placed in the crucible with the zircon side down. The length of time necessary to etch the zircons varies. Purple Precambrian zircons were etched in 15 minutes, whereas colorless Oligocene zircons required 4 hours in the etching solution. Two mounts are prepared, and the first mount is given a 1.5-hour etching period, to gauge the amount of time necessary to etch the zircon. If no tracks are found after 1.5 hours, the grains are placed in fresh etching solution for 1 to 2 hours more; if the sample is overetched, the other mount is then etched for a shorter time, usually 15 to 45 minutes, depending on the degree of overetching.

The epoxy mount is dissolved in the process of etching; therefore, the grains must be recovered and remounted for irradiation with neutrons. The zircons are embedded in Lexan by placing them on a glass slide which is then heated to  $190^\circ\text{C}$ . A small square of Lexan is then pressed on top of the zircons. The zircons embedded in Lexan plastic are placed next to an external detector of muscovite (4) and placed in a reactor for neutron irradiation. After irradiation the fossil tracks are counted in the zircon, and the induced tracks are counted in the muscovite detector.

The NaOH etch technique was used successfully to determine the zircon age for the Inconolable Granodiorite of California by fission tracks. The results agree with the K-Ar age determined from hornblende from the same gra-

Table 1. Mineral ages from the Inconolable Granodiorite (MG-3).

Mineral	Fission track* (million years)	K-Ar (million years)
Zircon		
Grain 1	$97 \pm 10$	
Grain 2	$100 \pm 10$	
Apatite (5)	$91 \pm 9$	
Hornblende (4)		98
Biotite (4)		87

\*  $\lambda_T = 7.03 \times 10^{-17} \text{ yr}^{-1}$  (8); a glass standard was used as a flux monitor.

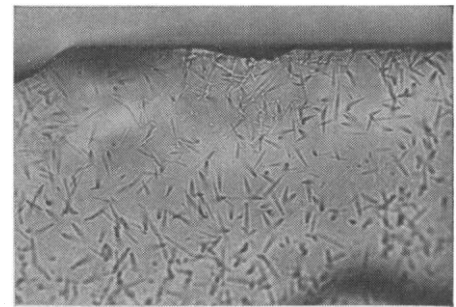


Fig. 1. Fission tracks in a zircon from the Inconolable Granodiorite of California, etched by sodium hydroxide solution heated to  $220^\circ\text{C}$  for 2 hours. The field of view is approximately  $60 \times 90 \mu$ .

nodiorite (Table 1). A discordancy between K-Ar ages on the hornblende and biotite is paralleled by a similar discordancy in fission-track ages between zircons and apatite and can be accounted for by their dissimilar annealing properties. As the annealing temperature of zircon is higher than that of apatite (1, 6), one would expect that, if the fission track ages of coexisting zircons and apatite are different, the zircon would be older.

C. W. NAESER

*Astrogeologic Studies Branch,  
U.S. Geological Survey,  
Menlo Park, California 94025*

### References and Notes

- R. L. Fleischer, P. B. Price, R. M. Walker, *J. Geophys. Res.* **70**, 1497 (1965).
- , *ibid.* **69**, 4885 (1964).
- C. W. Naeser, *Bull. Geol. Soc. Amer.* **78**, 1523 (1967).
- R. L. Fleischer, C. W. Naeser, P. B. Price, R. M. Walker, U. B. Marvin, *Science* **148**, 629 (1965).
- R. W. Kistler, P. C. Bateman, W. W. Brannock, *Bull. Geol. Soc. Amer.* **76**, 155 (1965).
- C. W. Naeser and F. C. W. Dodge, *ibid.*, in press.
- C. W. Naeser and H. Faul, *J. Geophys. Res.* **74**, 705 (1969).
- J. H. Roberts, R. Gold, R. J. Armani, *Phys. Rev.* **174**, 1482 (1968).
- I thank K. F. Fox and F. C. W. Dodge (U.S. Geological Survey) and R. L. Fleischer (General Electric Company) for assistance in experimentation and preparation of this report. Publication authorized by the director, U.S. Geological Survey.

14 April 1969